A State Estimator Using SCADA and Synchronized Phasor Measurements

Vedran Kirinčić

vedran.kirincic@riteh.hr

Srđan Skok

srdjan.skok@riteh.hr

Dubravko Franković

dubravko.frankovic@riteh.hr

University of Rijeka,
Faculty of Engineering, Department of Power Systems
Vukovarska 58, 51000 Rijeka, Croatia

Abstract – *A state estimator is presented, in which conventional measurements from the SCADA system and synchrophasors available from Phasor Measurement Units (PMUs) are used. A recursive algorithm for the part of the system observable by PMUs is applied, in which multiple sets of synchrophasors are processed. The obtained state estimate is then used together with SCADA measurements in an iterative procedure to estimate the state of the entire power system. The developed methodology was tested on IEEE test systems with 30 and 57 buses as well as on the model of the Croatian transmission system. The proposed solution is comparable in convergence with the classical state estimator and other hybrid models, whereas it enhances state estimation accuracy and filtering of measurement errors.*

1. INTRODUCTION

In addition to energy market development, which resulted in treating electrical energy as any other tradable good, integration of distributed generation introduces additional uncertainties in power system operation. A combination of lagging investments into the main infrastructure, due to either economical or environmental issues, with continuous focus on increased profits, often results in power system operation closer to its stability limits. Consequently, large power system blackouts in the last decade have further shifted attention and funding towards development and deployment of solutions based on emerging technologies. It is envisaged that the application of the synchronized measurement technology on top of the obsolete infrastructure would help Transmission System Operators (TSO) to cope with the ongoing challenges. Not only have the TSOs worldwide started to popularize their transmission systems with Phasor Measurement Units (PMUs), but the applications using measured synchrophasors of voltage and current have also been developed. Complex solutions are tailored to the parts of the power system and adjusted according to customer needs in order to preserve power system stability and integrity [1].

The cornerstone application in the control room that is expected to benefit from the utilization of synchrophasors is the power system state estimator. Since the estimated state of the power system is used as an input for other applications crucial for power system operation, such as power flow calculation and contingency analysis, many researchers have been focused on the improvement of state estimator performance [2]-[3]. Due to availability of highly redundant SCADA measurements and a gradual increase in the number of PMUs deployed in the power system, an evolutionary approach has been chosen by many utilities and hybrid state estimators were recognized as a solution how to integrate synchrophasors into state estimation practice [4].

A literature review reveals that there are several aspects in which state estimation can be enhanced, such as the accuracy of the estimated state, filtering of measurement errors as well as the speed and convergence of the algorithm applied [5]. In the state estimator proposed in [6], a set of constraints is introduced rather than transforming measurements, which would result in the propagation of measurement uncertainties. Another approach, which is given in [7], focuses on avoiding convergence issues by using phasors for the current in rectangular coordinates. Pseudo-voltages based on measured synchrophasors and the known parameters of branches are calculated in [8], while pseudo-flows and pseudo-injections are used as parts of measurement vectors in the state estimators given in [9]-[11], respectively. Although optimal PMU placement methods present an important part of state estimation prac-
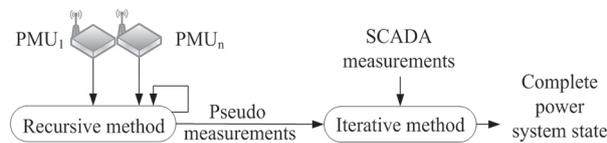
tice, they are not the focus of this paper, and therefore, an interested reader is advised to refer to [12].

The paper presents a state estimator in which synchrophasors are preprocessed in a recursive algorithm to take the advantage of their high sampling frequency. The obtained estimate for the part of the system observable by PMUs is then merged with SCADA measurements to estimate the state of the entire power system. The proposed methodology was applied to the IEEE test systems with 30 and 57 buses as well as the model of the Croatian transmission system. In order to validate its performance, the results of the proposed state estimator were compared with the results of the classical state estimator and other hybrid models.

The developed solution is explained in Section 2. Case studies and results obtained from simulations are given in Sections 3 and 4, respectively. Section 5 concludes the paper.

2. HYBRID STATE ESTIMATOR FORMULATION

The architecture of the proposed method consists of preprocessing the synchrophasors and state estimation of the entire power system. First, the recursive algorithm is used, with the measurement vector comprised of synchrophasors only, while the state vector comprises voltage angles and magnitudes only of those buses that are observable by PMUs deployed in the power system. The algorithm runs several times, each time with the newest set of synchrophasors. The result from the last run, which presents the estimated state of the part of the system observable by PMUs, is forwarded to the second part of the proposed state estimator. The second part of the solution is based on the iterative method. The measurement vector is formed from pseudo-measurements obtained in the first part and SCADA measurements. Since the state vector of this part comprises the states of all buses in the system, the result is the estimated state of the entire power system. The architecture of the developed solution is given in Figure 1.
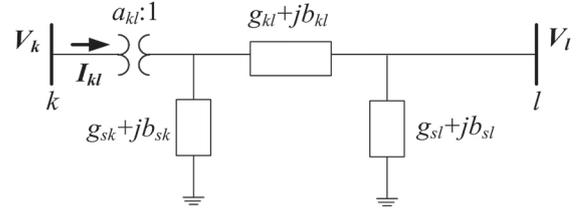

Fig. 1. The architecture of the proposed state estimator

The first part of the proposed model uses the state vector in polar coordinates, with voltage magnitudes and angles of the buses observable by PMUs:

$$\mathbf{x}_{Sync} = \begin{bmatrix} \mathbf{X}_{PMU}, \ \mathbf{X}_{Adjacent} \end{bmatrix}^T, \tag{1}$$

where $\mathbf{X}_{PMU}$ is the subset of voltage phasors at the buses with PMUs deployed and $\mathbf{X}_{Adjacent}$ is the subset of voltage phasors at the buses adjacent to PMU buses.

Figure 2 gives a pi-model of the network branch with tap modeling, where a is the off-nominal tap position of the transformer (for a transmission line $a = 1$), whereas g and b are branch conductance and susceptance, respectively. If a PMU is deployed at bus k, the voltage phasor $\mathbf{V}_k$ at bus k and the current phasor $\mathbf{I}_{kl}$ between the buses k and l are measured.

Fig. 2. A pi-model of the network branch with tap modeling

When there are more PMUs deployed in the system, the sets of voltage and current phasors are measured. Here, it is assumed that the number of measurement channels of each PMU is sufficient to measure the voltage phasor at the PMU bus and current phasors on all branches emerging from the PMU bus. The sets of voltage and current phasors measured by one PMU make an observable island that consists of the PMU bus and the adjacent buses. There is an indirect connection between voltage phase angles θ_k at N buses in the island, since all of them refer to a common angle reference θ_0 of the slack bus:

$$\theta_k = \theta_k - \theta_0, \quad \forall k \in \left\{ 1, ..., N \right\}. \tag{2}$$

The measurement vector of the state estimator used in the first part of the proposed solution consists of the set of voltage phasors in polar coordinates and the set of current phasors in rectangular coordinates:

$$\mathbf{z}_{Sync} = \begin{bmatrix} \mathbf{V}_{kPolar}, \mathbf{I}_{klRect} \end{bmatrix}^T = \begin{bmatrix} \begin{bmatrix} \theta_{kAng} \\ \mathbf{V}_{kMag} \end{bmatrix}, \begin{bmatrix} \mathbf{I}_{klR} \\ \mathbf{I}_{klI} \end{bmatrix} \end{bmatrix}^T. \tag{3}$$

Here, θ_{kAng} and $\mathbf{V}_{kMag}$ are the vectors of voltage magnitudes and angles, respectively, that are combined into the vector $\mathbf{V}_{kPolar}$. The current phasor $\mathbf{I}_{klRect}$ comprises real $\mathbf{I}_{klR}$ and imaginary $\mathbf{I}_{klI}$ parts of the measured currents. Due to the transformation of current phasors from polar to rectangular coordinates, one should calculate the uncertainties of the obtained values. Therefore, classical uncertainty propagation theory is used to derive standard deviations σi_R and σi_I of the real and imaginary parts of current phasors [13]:

$$\sigma_{i_R} = \sqrt{\left(\frac{\partial i_R}{\partial \phi} \right)^2 \sigma_\phi^2 + \left(\frac{\partial i_R}{\partial I} \right)^2 \sigma_I^2} = \sqrt{\left(I \sin \phi \right)^2 \sigma_\phi^2 + \left(\cos \phi \right)^2 \sigma_I^2}, \tag{4}$$

$$\sigma_{i_I} = \sqrt{\left(\frac{\partial i_I}{\partial \phi} \right)^2 \sigma_\phi^2 + \left(\frac{\partial i_I}{\partial I} \right)^2 \sigma_I^2} = \sqrt{\left(I \cos \phi \right)^2 \sigma_\phi^2 + \left(\sin \phi \right)^2 \sigma_I^2} \tag{5}$$

where σ_θ and σ_I are standard deviations of current angles and magnitudes, respectively.

While the relationship between voltage phasors and state vector elements is straightforward, the real and imaginary parts of current phasors are related to state vector elements as follows:

$$I_{klR} = b_{kl}V_l \sin\theta_l - g_{kl}V_l \cos\theta_l + V_k G \cos\theta_k - V_k B \sin\theta_k , \quad (6)$$

$$I_{klI} = -b_{kl}V_l \cos\theta_l - g_{kl}V_l \sin\theta_l + V_k B \cos\theta_k + V_k G \sin\theta_k , \quad (7)$$

where $B = b_{kl} + b_{sk}$, $G = g_{kl} + g_{sk}$.

Having a nonlinear measurement model due to measurements of currents, for the time instant k, the measurements and the states are related as follows:

$$z_k = h(x_k) + r_k, \quad (8)$$

where $h(x_k)$ is a set of nonlinear equations and vector r represents white Gaussian measurement noise with the covariance matrix R.

System state transition is assumed by slow changes of loads in a minute range. A linear discrete time prediction model is used to capture the quasi steady-state behavior of the system at the time instant k:

$$xk = F_{k-1}x_{k-1} + g_{k-1} + q_{k-1}, \quad (9)$$

where q is white Gaussian noise of the prediction model with the covariance matrix Q. The vector g and the matrix F, which are used to relate system states x_k and x_{k-1}, are calculated by applying the online parameter identification technique [14]:

$$g_k = (1+\beta_k)(1-\alpha_k)\bar{x}_k - \beta_k a_{k-1} + (1-\beta_k)b_{k-1}, \quad (10)$$

$$F_k = \alpha_k(1+\beta_k)\cdot I, \quad (11)$$

where I is the identity matrix. Vectors a_k and b_k are given as follows:

$$a_k = \alpha_k x_k + (1-\alpha_k)\cdot\bar{x}_k, \quad (12)$$

$$b_k = \beta_k(a_k - a_{k-1}) + (1-\beta_k)\cdot b_{k-1}, \quad (13)$$

while α_k and β_k are constants taken in the range from 0 to 1.

After presenting the state and measurement models used for the proposed state estimator, what follows is a brief description of the procedure, a thorough overview of what is given in [15]-[16].

The recursive algorithm estimates the system state at the time instant k by using the system state from the previous time instant $k-1$ and the latest set of the measured synchrophasors. Rather than linearizing the nonlinear measurement model, in order to capture the mean and the covariance of the distribution of the state vector $\hat{x}_{k-1}$, the matrix of sigma points is calculated as:

$$\hat{X}_{k-1} = [\hat{x}_{k-1}\ldots\hat{x}_{k-1}] + \sqrt{3}[\mathbf{0}\ \sqrt{P_{\hat{x}_{k-1}}}\ -\sqrt{P_{\hat{x}_{k-1}}}], \quad (14)$$

where $P_{\hat{x}_{k-1}}$ is the associated covariance matrix. The matrix $\hat{X}_k$ is then obtained by evaluating sigma points through the prediction model, as given in (9). The predicted state mean vector and the covariance matrix are determined as follows [17]:

$$\bar{x}_k = \sum_{i=0}^{2n} W_i^m \hat{X}_k^i, \quad (15)$$

$$P_{\bar{x}_k} = \sum_{i=0}^{2n} W_i^c [(\hat{X}_k^i - \bar{x}_k)(\hat{X}_k^i - \bar{x}_k)^T] + Q_{k-1}, \quad (16)$$

where n is the number of states for the part of the system observable by PMUs, $\hat{X}_k^i$ is the i-th column of the matrix $\hat{X}_k$, whereas the values of weights W^m and W^c can be found in [18].

Sigma points are updated for the time instance k:

$$\bar{X}_k = [\bar{x}_k\ldots\bar{x}_k] + \sqrt{3}[\mathbf{0}\ \sqrt{P_{\bar{x}_k}}\ -\sqrt{P_{\bar{x}_k}}], \quad (17)$$

and then they are propagated through the nonlinear function given by (8) in order to obtain the matrix $\bar{Z}_k$. The mean of the propagated points is obtained as:

$$\mu_k = \sum_{i=0}^{2n} W_i^m \bar{Z}_k^i, \quad (18)$$

where $\bar{Z}_k^i$ is the i-th column of $\bar{Z}_k$. The measurement covariance matrix and the cross-covariance of the state and measurements are calculated as:

$$S_k = \sum_{i=0}^{2n} W_i^c [(\bar{Z}_k^i - \mu_k)(\bar{Z}_k^i - \mu_k)^T] + R_k, \quad (19)$$

$$C_k = \sum_{i=0}^{2n} W_i^c [(\bar{X}_k^i - \bar{x}_k)(\bar{Z}_k^i - \mu_k)^T]. \quad (20)$$

The estimated state and the covariance matrix at the time instant k are given as:

$$\hat{x}_k = \bar{x}_k + K_k(z_k - \mu_k), \quad (21)$$

$$P_{\hat{x}_k} = P_{\bar{x}_k} - K_k S_k K_k^T, \quad (22)$$

where $K_k = C_k S_k^{-1}$ is the filter gain. The estimated state is used at the next time instant $k+1$. The results obtained in the last run are used as pseudo-measurements for the state estimator that estimates the state of the entire power system.

Estimation of the entire power system is obtained by applying the iterative method. In addition to voltage magnitudes and power measurements from the SCADA system, the measurement vector includes pseudo-measurements obtained in the last run of the state estimator that preprocesses synchrophasors:

$$z = [V, P_{flow}, Q_{flow}, P_{inj}, Q_{inj}, z_{Pseudo}]^T. \quad (23)$$

With reference to Fig. 2, a nonlinear measurement model is used, since there is a nonlinear relationship of elements of the state vector x (voltage magnitudes V and angles θ at all system buses) with measurements of power flows (P_{kl} and Q_{kl}) and power injections (P_k and Q_k):

$$P_{kl} = \frac{V_k^2}{a_{kl}^2}(g_{sk} + g_{kl}) - \frac{V_k V_l}{a_{kl}}(g_{kl}\cos\theta_{kl} + b_{kl}\sin\theta_{kl}), (24)$$

$$Q_{kl} = -\frac{V_k^2}{a_{kl}^2}(b_{sk} + b_{kl}) - \frac{V_k V_l}{a_{kl}}(g_{kl}\sin\theta_{kl} - b_{kl}\cos\theta_{kl}), (25)$$

$$P_k = V_k \sum_{l=1}^{N} V_l (G_{kl} \cos \theta_{kl} + B_{kl} \sin \theta_{kl}), \qquad (26)$$

$$Q_k = V_k \sum_{l=1}^{N} V_l (G_{kl} \sin \theta_{kl} - B_{kl} \cos \theta_{kl}), \qquad (27)$$

where G_{kl} and B_{kl} are the elements of the nodal admittance matrix. The relationship between the measurement vector $\mathbf{z}$ and the state vector $\mathbf{x}$ is given as:

$$\mathbf{z} = \mathbf{h}(\mathbf{x}) + \mathbf{e}, \qquad (28)$$

where $\mathbf{h}(\mathbf{x})$ is a set of nonlinear equations and $\mathbf{e}$ is the vector of measurement errors with the covariance matrix $\mathbf{R}$ and the weight matrix $\mathbf{W}$:

$$\mathbf{W} = \mathbf{R}^{-1} = diag\left\{1/\sigma_1^2, ..., 1/\sigma_i^2, ..., 1/\sigma_m^2\right\}. \qquad (29)$$

Here, σ_i is the standard deviation of the i-th measurement and its inverse square is used at the measurement weight. By assuming a uniform probability distribution over the entire range of uncertainties, the standard deviation of each measurement is computed by using the maximum uncertainty Δu [13], [19]:

$$\sigma_i = \frac{\Delta u_i}{\sqrt{3}}, i = 1, ..., m, \qquad (30)$$

where m is the number of measurements.

Optimal estimation is obtained when the goal function $J(\mathbf{x})$ is minimized:

$$J(\mathbf{x}) = \frac{1}{2}[\mathbf{z} - \mathbf{h}(\mathbf{x})]^T \mathbf{R}^{-1}[\mathbf{z} - \mathbf{h}(\mathbf{x})]. \qquad (31)$$

As the measurement model is nonlinear, an iterative algorithm is applied and the change of the state vector elements $\Delta \mathbf{x}^k$ is computed in the k-th iteration:

$$\mathbf{G}(\mathbf{x}^k)\Delta \mathbf{x}^k = \mathbf{H}^T(\mathbf{x}^k)\mathbf{R}^{-1}[\mathbf{z} - \mathbf{h}(\mathbf{x}^k)], \qquad (32)$$

$$\Delta \mathbf{x}^k = \mathbf{x}^{k+1} - \mathbf{x}^k, \qquad (33)$$

where the gain matrix and the Jacobian matrix are given as follows:

$$\mathbf{G}(\mathbf{x}^k) = \mathbf{H}^T(\mathbf{x}^k) \cdot \mathbf{R}^{-1} \cdot \mathbf{H}(\mathbf{x}^k), \qquad (34)$$

$$\mathbf{H} = \partial \mathbf{h}(\mathbf{x}) / \partial \mathbf{x}. \qquad (35)$$

In order to avoid high weights for highly accurate measurements, such as zero-injections, which leads to ill-conditioning of the gain matrix and possible convergence issues [2], a set of constraints is introduced:

$$L(\mathbf{x}, \lambda) = \frac{1}{2}[\mathbf{z} - \mathbf{h}(\mathbf{x})]^T \mathbf{R}^{-1}[\mathbf{z} - \mathbf{h}(\mathbf{x})] - \lambda^T \mathbf{c}(\mathbf{x}) \qquad (36)$$

$$subject\ to\ \mathbf{c}(\mathbf{x}) = \mathbf{0},$$

where λ is the vector of Lagrange multipliers. Minimization of $L(\mathbf{x}, \lambda)$ is obtained by satisfying the first-order optimality conditions $\partial L(\mathbf{x},\lambda) / \partial \mathbf{x} = 0$ and $\partial L(\mathbf{x},\lambda) / \partial \lambda = 0$. Finally, by using the Gauss-Newton method the system of equations is iteratively solved for $\Delta \mathbf{x}$ and λ:

$$\begin{bmatrix} \alpha \mathbf{H}^T \mathbf{R}^{-1} \mathbf{H} & \mathbf{C}^T \\ \mathbf{C} & \mathbf{0} \end{bmatrix} \begin{bmatrix} \Delta \mathbf{x} \\ -\lambda \end{bmatrix} = \begin{bmatrix} \alpha \mathbf{H}^T \mathbf{R}^{-1}(\mathbf{z} - \mathbf{h}(\mathbf{x}^k)) \\ -\mathbf{c}(\mathbf{x}^k) \end{bmatrix}, \qquad (37)$$

where $\mathbf{C} = \partial \mathbf{c}(\mathbf{x}) / \partial \mathbf{x}$ and $\Delta \mathbf{x} = \mathbf{x}^{k+1} - \mathbf{x}^k$. The scaling factor $\alpha = 1 / \max(diag(\mathbf{R}^{-1}))$ is used to additionally minimize the gain matrix condition number. The stopping criterion for the iterative procedure is the value of $\Delta \mathbf{x}^k$ smaller than the desired tolerance.

3. CASE STUDIES

The proposed state estimator was applied to IEEE test systems with 30 and 57 buses [20] as well as a mathematical model of the Croatian transmission system. The results were compared with the results of the classical state estimator that uses only conventional SCADA measurements and other hybrid state estimators given in Table 1.

Table 1. State estimators

Abbreviation	Explanation	Ref.
Classic	Classical state estimator	[2]
HCSE	Hybrid Constrained State Estimator	[6]
RectI	Rectangular Currents State Estimator	[7]
SEPV	State Estimator with Pseudo Voltages	[8]
SEPF	State Estimator with Pseudo Flows	[9]
SEPM	State Estimator with Pseudo Measurements	[10]
SEPI	State Estimator with Pseudo Injections	[11]

3.1. LOCATIONS AND GENERATION OF MEASUREMENTS

For IEEE test systems, the locations of SCADA measurements were determined after observability analysis in order to ensure complete observability of the power system. The locations of PMUs were chosen by using redundancy analysis to enhance local redundancy levels, as given in Table 2 – Table 3. For the Croatian transmission system, real locations of measurements were used, as given in Figure 3.
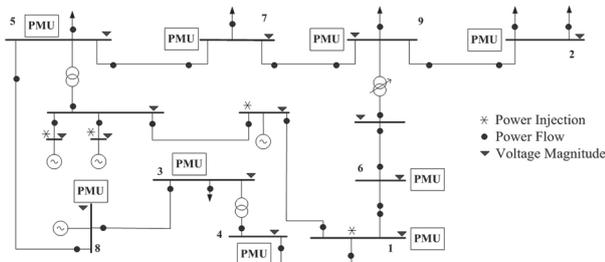
Table 2. Measurement locations for the IEEE 30 system

Measurement type	Measurement location
Voltage phasor (# bus)	1, 4, 5, 7, 9, 14, 15, 16, 17
Current phasor (#from-#to)	1-2, 1-3, 4-6, 5-7, 9-11, 9-10, 4-12, 14-15, 16-17, 15-18, 15-23, 4-2, 4-3, 5-2, 7-5, 7-6, 9-6, 14-12, 15-12, 16-12, 15-14, 17-16, 17-10
Voltage magnitude (#bus)	2, 3, 6, 9, 11, 14, 16, 17, 25, 30
Power flow (#from-#to)	1-3, 2-4, 2-6, 4-6, 5-7, 6-8, 6-9, 6-10, 12-13, 12-15, 14-15, 16-17, 15-18, 10-20, 10-17, 15-23, 25-26, 25-27, 28-27, 29-30, 6-28
Power injection (#bus)	1, 2, 4, 6, 10, 11, 12, 15, 18, 19, 24, 25, 27, 30

Standard uncertainties are computed by using expression (30) and the maximum measurement uncertainties that are usually known for each type of measurements and are given by equipment manufacturers, as shown in Table 4 [6], [21]. A set of true measurements was generated from the power flow calculation output, to which random Gaussian noise with a zero mean and given uncertainties was added in order to obtain noisy measurements.

Table 3. Measurement locations for the IEEE 57 system

Measurement type	Measurement location
Voltage phasor (# bus)	1, 3, 5, 8, 10, 11, 13, 14, 15, 16, 18, 41, 42, 57
Current phasor (#from-#to)	1-2, 3-4, 8-9, 13-14, 13-15, 1-15, 1-16, 1-17, 3-15, 5-6, 10-12, 11-13, 14-15, 18-19, 11-41, 41-42, 41-43, 15-45, 14-46, 10-51, 13-49, 11-43, 57-56, 3-2, 5-4, 8-6, 10-9, 11-9, 13-9, 14-13, 15-13, 15-1, 16-1, 15-3, 18-4, 18-4, 8-7, 13-11, 13-12, 16-12, 15-14, 41-11, 42-41, 41-56, 42-56, 57-39
Voltage magnitude (#bus)	1, 3, 4, 5, 7, 8, 11, 15, 17, 22, 27, 31, 37, 44, 52, 54
Power flow (#from-#to)	1-15, 1-17, 2-3, 3-4, 4-5, 4-18, 6-7, 7-8, 7-29, 8-9, 9-10, 9-11, 9-12, 9-13, 12-16, 12-17, 13-15, 14-15, 14-46, 18-19, 22-23, 22-38, 24-25, 28-29, 24-26, 26-27, 32-33, 35-36, 38-48, 46-47, 52-29, 52-53
Power injection (#bus)	1, 2, 5, 6, 10, 12, 13, 15, 18, 19, 25, 27, 30, 32, 35, 41, 43, 44, 47, 49, 51, 53, 54, 55, 57

Fig. 3. Measurement locations for the Croatian system

Table 4. Maximum measurement uncertainties

Synchrophasors		
Current magnitude	Voltage magnitude	Current and voltage phase angle
0.03%	0.02%	0.01°
SCADA measurements		
Voltage magnitude	Power flow	Power injection
0.2%	2%	2%

3.2. TRANSITION OF SYSTEM STATE

The estimators used in modern control rooms are rerun every few minutes, using the measurements collected during that period. Therefore, between the two runs of state estimators we assumed the time period of several minutes during which the values of loads on selected buses were increased following a linear trend from 5% up to 30%, with random fluctuation of 3% in value. Furthermore, the time period was divided into k_{max}= 50 time-sample subintervals and in each subinterval power flow calculation was run to obtain a different set of measurements due to a smooth change in load. To make simulation more realistic, generator outputs were changed according to the assignment of participation factors in order to avoid overload of the slack bus.

Since synchrophasors are sampled at a much higher frequency in comparison with SCADA measurements, the proposed model in the preprocessing stage used a new set of synchrophasors in each subinterval k. The state estimate obtained from the previous run in the subinterval $k-1$ was updated and the result was used to compute the state in the subinterval $k+1$. The state estimated for the part of the system observable by PMUs in the last subinterval of the whole simulation period was used as pseudo-measurements in the iterative state estimator that also takes SCADA measurements into the measurement vector and estimates the state of the entire power system. Since SCADA measurements do not have precise time tags such as synchrophasors, they were collected during the whole simulation period for all state estimators. Hybrid state estimators, with the exception of the proposed model, used the latest set of the measured synchrophasors and were run at the end of the simulation period.

The online parameter identification technique was initialized by using the first two samples of voltage magnitudes and angles from power flow calculation. As the initial states were assumed as highly accurate, the diagonal elements of the matrix P_0 were initialized to 10^{-6} and updated, while the diagonal elements of the matrix Q were set to the same value and remained constant during the whole simulation period [22]. The constants α and β were set to 0.8 and 0.5, respectively [13].

3.3. EVALUATION OF THE STATE ESTIMATOR PERFORMANCE

The results of the proposed state estimator were compared with the results obtained by applying other hybrid models and the classical state estimator. The results given in the section that follows were obtained by averaging the results of 100 Monte Carlo trials, each time with different random noise in measurements. The accuracy of state estimators was compared by calculating the variance of the estimated states of the entire power system:

$$\sigma_\Sigma^2 = \frac{1}{M} \sum_{j=1}^{L} \sum_{i=1}^{M} \left(\mathbf{x}(j) - \hat{\mathbf{x}}(j)_{(i)} \right)^2, \qquad (38)$$

where:

M is the number of Monte Carlo trials,

L is the number of state variables,

$\mathbf{x}$ is the vector of true state values, and

$\hat{\mathbf{x}}_{(i)}$ is the estimated state vector in the i-th Monte Carlo trail.

The filtering of measurement errors is presented through the filtering index $\xi(\hat{x})$ that was obtained as:

$$\xi(\hat{x}) = \frac{1}{M} \sum_{i=1}^{M} \frac{\sum_{j=1}^{m} \left(\hat{z}_j - z^{true}_j \right)^2}{\sum_{j=1}^{m} \left(z_j - z^{true}_j \right)^2}, \qquad (39)$$

where,

$\hat{z}$ are the calculated values based on the estimated state,

z are the noisy measurements,

z^{true} are the true values (without random errors), and

m is the number of measurements.

The number of iterations and the computation time needed to reach the convergence criterion of 10^{-6} were used as indicators of convergence and speed of state estimators.

4. RESULTS

What follows are the results obtained from simulations when state estimators were applied to test systems. Table 5 – Table 7 provide the results of the proposed solution (*HSE*) in comparison with the classical state estimator and other hybrid models.

Table 5. State estimation results for the IEEE 30 system

System	SE	σ_Σ^2	ξ	Iter.	Time [s]
IEEE 30	Classic	6.35 x 10⁻³	1.013	4.98	0.03
	HCSE	8.928 x 10⁻⁵	0.035	4.28	0.10
	Rectl	8.928 x 10⁻⁵	0.035	4.79	0.08
	HSE	*8.315 x 10⁻⁵*	*0.034*	*1+3.19*	*0.17+0.04*
	SEPV	8.826 x 10⁻⁵	0.161	4.19	0.05
	SEPF	8.448 x 10⁻⁵	0.035	4.28	0.06
	SEPM	8.475 x 10⁻⁵	0.035	4.36	0.07
	SEPI	1.356 x 10⁻⁴	0.146	4.73	0.03

When comparing the results of hybrid models with the results of a classical solution, it can be seen that the inclusion of synchrophasors into the measurement vector enhances state estimation accuracy and the filtering of measurements errors. Furthermore, from the results obtained, it can be concluded that, in comparison with other hybrid models [6]-[11], the proposed model additionally enhances state estimation accuracy

and the filtering of measurement errors, since it provides the smallest values of the variance of estimated states of the entire power system and of the filtering index. Therefore, it is clear that a modification of the measurement vector in comparison to the models given in previous publications, results in enhancement of hybrid state estimator performance.

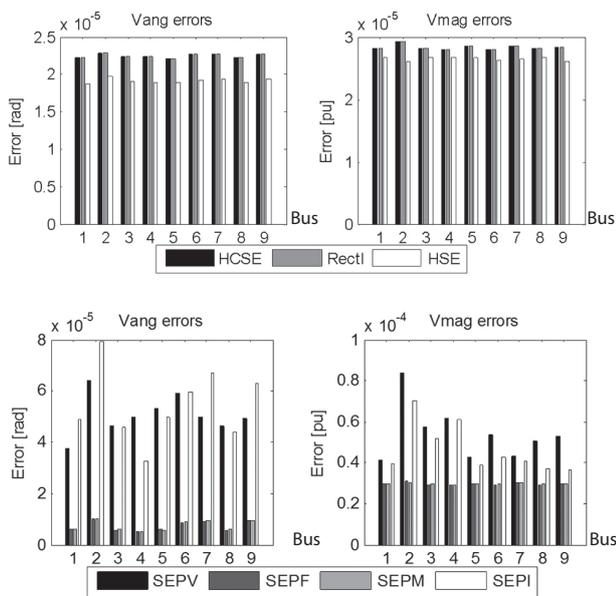**Table 6.** State estimation results for the IEEE 57 system

System	SE	σ_Σ^2	ξ	Iter.	Time [s]
IEEE 57	Classic	4.553 x 10⁻³	0.944	5.02	0.08
	HCSE	8.826 x 10⁻⁵	0.036	4.97	0.35
	Rectl	8.837 x 10⁻⁵	0.036	5.00	0.13
	HSE	*4.038 x 10⁻⁵*	*0.013*	*1+3.00*	*0.47+0.06*
	SEPV	7.228 x 10⁻⁵	0.066	4.30	0.10
	SEPF	1.023 x 10⁻⁴	0.041	4.98	0.12
	SEPM	1.045 x 10⁻⁴	0.044	5.00	0.12
	SEPI	1.214 x 10⁻⁴	0.091	4.71	0.10

Table 7. State estimation results for the Croatian system

System	SE	σ_Σ^2	ξ	Iter.	Time [s]
CRO	Classic	1.435 x 10⁻⁵	0.322	4.00	1.94
	HCSE	3.819 x 10⁻⁶	0.055	4.00	3.05
	Rectl	3.819 x 10⁻⁶	0.055	4.00	2.70
	HSE	*3.766 x 10⁻⁶*	*0.055*	*1+2.83*	*0.53+1.42*
	SEPV	6.099 x 10⁻⁶	0.106	4.00	2.70
	SEPF	3.778 x 10⁻⁶	0.055	4.00	2.15
	SEPM	3.782 x 10⁻⁶	0.056	4.00	2.15
	SEPI	8.320 x 10⁻⁶	0.161	4.00	2.01

When comparing the results of hybrid models with the results of a classical solution, it can be seen that the inclusion of synchrophasors into the measurement vector enhances state estimation accuracy and the filtering of measurements errors. Furthermore, from the results obtained, it can be concluded that, in comparison with other hybrid models [6]-[11], the proposed model additionally enhances state estimation accuracy and the filtering of measurement errors, since it provides the smallest values of the variance of estimated states of the entire power system and of the filtering index. Therefore, it is clear that a modification of the measurement vector in comparison to the models given in previous publications, results in enhancement of hybrid state estimator performance.

The computation time and the number of iterations for the proposed solution are given in two parts. Preprocessing of synchrophasors is shown as a single iteration, whereas the second part presents the number of iterations of the second method. Regarding the computation time, a classical state estimator is the fastest one due to its simplicity and the smallest number of measurements, as only SCADA measurements are used.

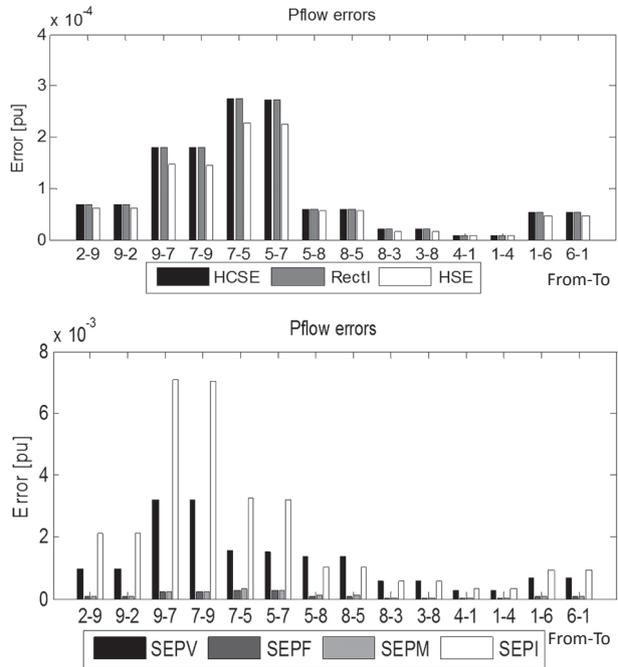**Fig. 4.** Estimation errors for the Croatian power system

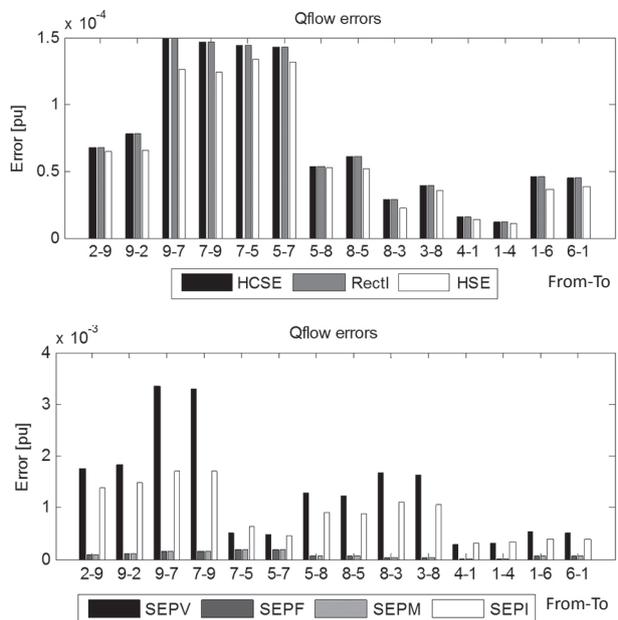**Fig. 5.** Power injection errors for the Croatian system

Although the computation time of the proposed state estimator is slightly larger due to processing of multiple sets of synchrophasors in comparison with other models that use only one set of measurements, it is still within acceptable time limits, which is confirmed by the smallest number of iterations necessary to reach the convergence criterion.

Due to space limitations, the results are visualized for the model of the Croatian power system only. As the complete mathematical model of the Croatian transmission system comprises 110 kV, 220 kV and 400 kV voltage levels, with 200 buses and 287 branches in total, the results are given for the part of the system that is observable by PMUs. Estimation errors for the buses with the deployed PMUs are given in Figure 4. Errors of calculated power injections and flows are given in Fig. 5 - Fig. 7, respectively. In these figures, the results for the classical state estimator are not presented, since high values of its errors would

make the results of hybrid state estimators unreadable. In comparison with other models, the proposed method provides the smallest errors of the estimated voltage magnitudes and angles on the buses equipped with PMUs. Furthermore, estimation of the power system state which is more accurate results in the calculation of power injections and power flows that are also more accurate.

Fig. 6. Active power flow errors for the Croatian system

Fig. 7. Reactive power flow errors for the Croatian system

5. CONCLUSIONS

The paper presents the state estimator that uses both conventional SCADA measurements and synchrophasors available from PMUs. The methodology uses multiple sets of synchrophasors in order to take advantage of their high sampling frequency and precise time tags.

After synchrophasors are preprocessed in the recursive algorithm, the state estimate for the part of the system observable by the PMU is forwarded to the iterative procedure, where SCADA measurements are also taken into the measurement vector and the state of the entire power system is estimated.

In order to test its performance for power systems of different sizes, topologies and the number of measurements, the developed solution was applied to IEEE test systems with 30 and 57 buses. Additionally, as an example of the real power system, the mathematical model of the entire Croatian transmission system was used, with actual locations of SCADA measurements and PMUs. After running 100 Monte Carlo simulations, the averaged results were compared with the results of the classical state estimator and other hybrid models. Performance indices were computed to investigate estimation accuracy and filtering of measurement errors as well as convergence and speed of computation.

When compared with other state estimators, the developed model enhances state estimator accuracy that leads towards increased accuracy of the calculation of power injections and flows. Furthermore, filtering of measurement errors for all test systems is also improved. Although the computation time of the given estimator is slightly larger in comparison with other methods, it is still within acceptable time limits. The latter is supported by the smallest number of iterations. The enhancement of state estimator performance by applying the proposed model offers a useful tool for the power system operator to operate the power system economically, while preserving power system stability and integrity.

6. REFERENCES

[1]   S. Chakrabarti, E. Kyriakides, B. Tianshu, D. Cai, V. Terzija, "Measurements get together" IEEE Power and Energy Magazine, Vol. 7, 2009, pp. 41-49.

[2]   A. Abur, A. Gomez-Exposito, "Power System State Estimation: Theory and Implementation", Marcel Dekker, 2004.

[3]   A. Monticelli, "State Estimation in Electric Power Systems: A Generalized Approach", Kluwer Academic Publishers, 1999.

[4]   A. Phadke, J. Thorp, "Synchronized phasor measurements and their applications", Springer, 2008.

[5]   "Metrics for Determining the Impact of Phasor Measurements on Power System State Estimation", KEMA, Arnhem, The Netherlands, 2006.

[6]   G. Valverde, S. Chakrabarti, E. Kyriakides, V. Terzija, "A constrained formulation for hybrid state esti-

mation", IEEE Transactions on Power Systems, Vol. 26, 2011, pp. 1102-1109.

[7]   T. S. Bi, X. H. Qin, Q. X. Yang, "A novel hybrid state estimator for including synchronized phasor measurements", Electric Power Systems Research Vol. 78, 2008, pp. 1343-1352.

[8]   S. Chakrabarti, E. Kyriakides, G. Valverde, V. Terzija, "State estimation including synchronized measurements", Proceedings of the IEEE Power Tech conference, Bucharest, Romania, 2009, pp. 1-5.

[9]   M. Asprou, E. Kyriakides, "Enhancement of hybrid state estimation using pseudo flow measurements", Proceedings of Power and Energy Society General Meeting, Detroit, USA, 2011, pp. 1-7.

[10]   V. Kirincic, S. Skok, V. Terzija, "A Hybrid State Estimator with Pseudo-Flows and Pseudo-Injections", International Review on Modelling and Simulations Vol. 6, 2013, pp. 218-226.

[11]   V. Kirincic, S. Skok, A. Marusic, "A Hybrid Constrained State Estimator with Pseudo Injection Measurements", Przegląd Elektrotechniczny, Vol. 89, 2013, pp. 137-142.

[12]   N. M Manousakis, G. N. Korres, P. S.Georgilakis, "Taxonomy of PMU Placement Methodologies", IEEE Transactions on Power Systems, Vol. 27, 2012, pp. 1070-1077.

[13]   ISO-IEC-OIML-BIPM, "Guide to the Expression of Uncertainty in Measurement", 1992.

[14]   A. M. Leite da Silva, M. B. Do Coutto Filho, J. F. de Queiroz, "State forecasting in electric power systems", IEE Proceedings on Generation, Transmission and Distribution. Vol. 130, 1983, pp. 237-244.

[15]   G. Valverde, V. Terzija, "Unscented Kalman filter for power system dynamic state estimation" IET Gen., Transm. & Dist., Vol. 5, 2011 pp. 29-37.

[16]   G. Valverde "Uncertainty and state estimation of power systems", The University of Manchester, School of Electrical and Electronic Engineering, UK, PhD Thesis, 2012.

[17]   S. Sarkka, "On unscented Kalman filtering for state estimation of continuous-time nonlinear systems", IEEE Trans. Autom. Control, Vol. 52, 2007, pp. 1631–1641.

[18] D. Simon, "Kalman, H infinity, and Nonlinear Approaches", John Wiley & Sons, Inc., 2006.

[19] S. Chakrabarti, E. Kyriakides, M. Albu, "Uncertainty in Power System State Variables Obtained Through Synchronized Measurements", IEEE Transactions on Instrumentation and Measurement, Vol. 58, 2009, pp. 2452-2458.

[20] R. Christie, Power system test archive, http://www.ee.washington.edu/research/pstca (accessed 2016].

[21] Model 1133A GPS-Synchronized Power Quality/Revenue Standard, Arbiter Systems, Inc. CA, USA.

[22] S. Chun-Lien, L- Chan-Nan, "Interconnected network state estimation using randomly delayed measurements", IEEE Transactions on Power Systems, Vol. 26, 2001, pp. 870-878.